International Journal of Nanoelectronics and Materials
Volume 16, No. 4, October 2023 [933-946]

Performance of Multifarious Active Layer Materials in Organic Photovoltaic Cells: A Review

Karthika Krishnakumar[1*], Ashish Grover[2] and Pardeep Kumar[3]

[1]Department of Electronics and Communication Engineering, MRIIRS, Faridabad, Haryana, India
[2]Department of Electrical and Electronics Engineering, MRIIRS, Faridabad, Haryana, India
[3]Pro Vice Chancellor, MRIIRS, Faridabad, Haryana, India

Received 1 July 2022, Revised 16 November 2022, Accepted 30 May 2023

ABSTRACT

When humans understood the importance of solar energy for the future, they will pursue the development of polymer photovoltaic cells, which offered numerous benefits than ordinary photovoltaic cells. Multifarious polymers are commonly used for active layers in Organic Photovoltaic (OPV) cells. In this research review study, focus was made on the works during recent past years involving three polymers: PM6:Y6, PIF8BT:PDI and PBDB-T:ITIC as separate active layers, and their photovoltaic aspects were characterized. The efficiency outputs in each case were studied and the best efficiency outputs along with other photovoltaic aspects were highlighted. It was found that in ternary or quaternary device architectures, OPV cells with active layers of PBDB-T:ITIC and PM6:Y6 exhibited substantial efficiency. Having discussed several factors which can optimize the performance of these OPV cells, it is proffered that these OPV cells can be upscaled from lab to practical level efficiently.

Keywords: Active layer, Inverted topology, Organic Photovoltaic (OPV) cell, Polymer.

1. INTRODUCTION

A solar cell, also known as a photovoltaic (PV) cell, is a device that transforms the energy of light directly into electrical energy via the photovoltaic effect, a physical and chemical phenomena [1]. PV cells are typically grouped into four generations based on the time and material categories employed in their manufacture [2]. Organic Photovoltaic (OPV) cells belong to the third era of PV cells [3]. It is also referred to as a polymer PV cell or a plastic PV cell [4]. Organic PV cell has acquired ubiquity lately because of its benefits like minimal expense, adaptability, lightweight, and haziness [5]. In 1839, Becquerel discovered the photovoltaic peculiarity, namely the photoelectrochemical effect. In the review, photocurrent was recognized by enlightening silver halogen-covered platinum electrodes in a watery course of action [6]. After a significant period, in 1873, Smith confirmed photoconductivity in high resistance metal bars (se) [7], and in 1906, Pochettino reported the principal finding of photoconductivity in anthracene, an organic compound [8]. Calvin, in 1958, created the first OPV cell based on magnesium phthalocyanine (MgPc), achieving open-circuit voltage (Voc) of 200mV [9]. Later, Morel et al. synthesized Al/MgPc/Ag cell, and a 0.01% energy conversion efficiency was reported at wavelength of 690 nm [10]. Tourillon et al. suggested an Al/poly(3-methyl-thiophene)/Pt OPV cell with a fill factor = 0.3 %, open-circuit voltage = 0.4V, along with an External Quantum Efficiency (EQE) = 0.17 % [11]. Halls, J. J. et al. created an organic cell with a bis-perylene electron donor layer (EDL) over which produced a poly(p – phenylenevinylene) PPV layer, bringing about a pinnacle 6% EQE and 1% Power Conversion Efficiency (PCE) [12]. The operating concept of an OPV cell can be stated in four basic phases, which are shown below:

* Corresponding author: karthikakrishnakumar18752@gmail.com

- Incident light absorption: An OPV cell will absorb light with a sufficiently high energy level. The electrons get excited from the highest occupied molecular orbital (HOMO) to the lowest unoccupied molecular orbital (LUMO), bringing about the arrangement of an exciton. In the event that the energy of the assimilated light surpasses the band gap, then the rot down of electrons at an energy level higher than the LUMO will take place. Thus, energy is squandered as heat, and the action called "thermalization" happens. In photovoltaics, significant source of energy waste is thermalization [13].
- Exciton diffusion: At the point when an electron-hole pair is shaped, this starts diffusing to the donor acceptor juncture across all OPV cell parts. Here, exciton dissociation is caused by the offset between LUMO levels. This must happen within a specific time frame, otherwise a process called "recombination" will take place. The lifespan of an exciton is about 10 nm. The lifetime or life span of the exciton refers to the distance that the exciton may spread in this period [13].
- Exciton dissociation: Electrons move towards the acceptor at the interface, while the hole remains on the donor. Attraction of these charge carriers forms a charge-transfer state and, as the distance between the charge carriers grows, the attraction between them reduces. Finally, it results in a state of charge-separation as thermal energy overcomes the binding energy of the charge carriers. Therefore, recombination occurs at the interface [13].
- Charge-carrier transport and collection: Now carriers disseminate to the apt electrodes through the concerned interfacial layers, and finally, these charge carriers will be collected at the electrodes. Consequently, these are used to produce current [13].

The OPV cells are of two types, normal and inverted based on layer stack topology. The OPV cells are built of different layers namely, two outer electrodes out of which one is transparent, hole transport layer (HTL), electron transport layer (ETL), and active/dynamic material. Figure 1 shows the correct sequence of various layers in a normal OPV cell structure, i.e., substrate/anode/HTL/active layer/ETL/cathode. In its inverted topology, the arrangement of an OPV cell is such that the anode and cathode flip along with ETL and HTL, i.e., substrate/cathode/ETL/active layer/HTL/anode. The dynamic material in a PV cell acts as a semiconductor, i.e., it contains both conductor and insulator with a band gap in between. Band gap is mainly of two types, direct and indirect band gaps. For example, silicon (Si) is a commonly used indirect band gap material. For exciting an electron from valance band (V.B) to conduction band (C.B), it requires lattice vibration. This reduces the likelihood of transition and necessitates a thicker slab of materials. In such cases, organic materials with direct band gap come into play. Active layer consists of two layers namely the donor and acceptor, which are made of polymers, play a very important role in OPV cells. The reference device geometry is utilized to fabricate OPV cells in both lab-scale size and complete solution processing.

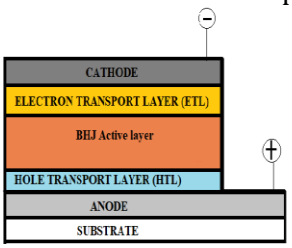

Figure 1. Schematic diagram of OPV cell.

In recent decades, researchers have been behind the creation of novel photovoltaic materials, hence there is a rapid progress in the attainment of PCEs in OPV cells [5]. This review focuses primarily on three active layer materials, namely PM6:Y6, PIF8BT:PDI, and PBDB-T ITIC based OPV cells. This analysis is separated into three sections; first, we discuss the PM6:Y6 based OPV

cells, then followed by the PIF8BT:PDI and PBDB-T:ITIC based OPV cells. Finally, an analogy between the three materials mentioned above is also discussed.

2. PM6:Y6 BASED OPV CELLS

The PM6:Y6 is also known as PBDB-TF or PBDB-T2F. PM6:Y6-constructed devices have received considerable attention. It is a D–π–A copolymer in which D, π and A units are benzodithiophene (BDT), thiophene, and benzodithiophene-4,8-dione (BDD), respectively. Figure 2 shows the subatomic structure of acceptor Y6 and donor PM6. The HOMO energy of PM6:Y6 is E ≈ 5.50 eV, as well as an optical bandgap (Eg^{opt})≈ 1.80 eV. The PM6 can be blended with a wide range of Non-fullerene Acceptors (NFAs), including small molecules and polymers. Accordingly, PM6 was demonstrated to be a decent polymer donor. This PM6:Y6 research review intends to keep academics up to date on recent developments and give inspiration for future high-performance OPV cell development. The Voc, short circuit current density(Jsc), and fill factor (FF) values of PM6:Y6-based OPV cells have been carefully analysed to understand the fundamental basis of their remarkable performance [5]. Yuan et al. synthesized OPVs in both conventional and inverted topologies. In this study, a neoteric class of NFA (Y6) with an Eg^{opt} of 1.81 eV was discovered. The PCE of the device architectures ITO/PEDOT:PSS/PM6:Y6/PDINO/Al (conventional) and ITO/ZnO/PM6:Y6/MoO3/Ag (inverted) were both 15.7 %. At 100 nm, the conventional structure with Eg^{opt} = 1.33 eV attained PCE of 15.3 %, Voc of 0.86 V, Jsc of 24.3 $mAcm^{-2}$, and FF of 73.2 %. After thermal annealing at 110 ℃ with additive 1-chloronapthalene (CN) of 0.5% for 10 minutes, the optimized PM6:Y6-based device obtained PCE of 15.7 %, Voc of 0.83 V , Jsc of 25.3 $mAcm^{-2}$, along with FF of 74.8 %. With the accretion of dynamic layer thickness to 250 nm, PCE, Voc, and FF were all reduced marginally, although Jsc rose. Inverted structure of Eg^{opt} = 1.33 eV at 100 nm achieved PCE of 15.7 %, Voc of 0.82 V , Jsc of 25.2 $mAcm^{-2}$, and FF of 76.1 %. This investigation also revealed that Y6-based devices attain PCE of 13.6 % at 300 nm [14].

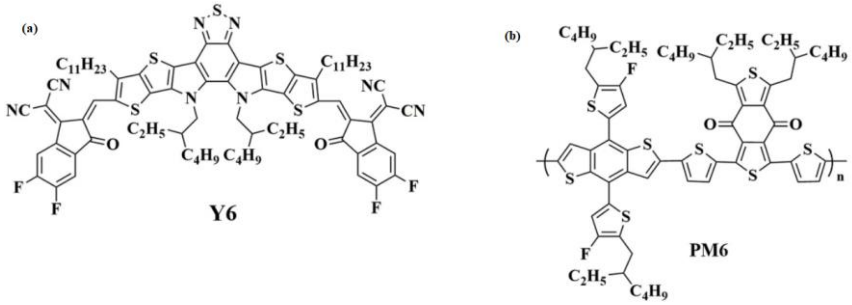

Figure 2. (a) Acceptor Y6 subatomic structure [5]. (b) Donor PM6 subatomic structure [5]

Subsequently, the research done by Karki et al. gives information on the device's structure and morphology. An OPV cell with a single junction was built in this study and found to have more than 15% PCE. An ITO (Indium Tin Oxide)/ PEDOT: PSS /PM6:Y6/PDINO/Al (Aluminium) device structure was utilized. During this investigation, the different factors that determine the PCE, Voc, FF, and Jsc were thoroughly analyzed and noted. Finally, this investigation demonstrated that the loss of radiative and non-radiative recombination was low (0.485 eV). The blend used in the study also has a minimum energetic disturbance, which contributes to even lower voltage losses. This research reveals that PCEs more than 15 % require modest voltage losses, average levels of 'non-geminate recombination', and extraction of charge for the majority of the device's relevant operating conditions [15].

Zhang et al. developed a technique for thermal doping. P-dopants in this study were made with the Lewis acid BCF $(C_6F_5)_3B$. The above made the OPV cells more efficient by 16.0 % over PM6:Y6 based OPV cells [16].

Pan et al. used only a minimal quantity of PCBM to get 16.7 % efficiency in the PM6:Y6 OPV cell. The use of PM7:Y6, PM6/IT-4F, PM6:Y6, and PM7/IT-4F as active layer materials was the primary focus of this study. The PC71BM, as an additive material, was used in all of the active layer components indicated above. The PCEs amounted to 15.4 %, 13.4 %, 15.5 %, and 13.1 %, respectively [17].

Yang et al. actualized an extraordinary PCE of 16.8% by incorporating a new acceptor material (PIDTCT) with thiophene-fused end groups onto PM6Y6-based OPV cell [18].

Tokmoldin et al. studied PV cells to determine the short-circuit current's independence from the concentration of the photoactive layer. This research shows a variety of optoelectronic evaluations, such as mobility measurements, charge extraction by linearly increasing voltage, photoinduced absorption spectroscopy, Mott–Schottky analysis, and AFORS-HET simulations. These evaluations conclude that the constant photocurrent for gadgets with various dynamic layer thicknesses is connected to the Y6's dispersion length surpassing 300 nm. The findings show that the key role is played by diffusion transport. This makes PM6:Y6 OPV cell, which is doped, operates similarly to normal PV cells. It is supposed to be a basic essential for the construction of such a long-haul thick OPV cell, proficient, and high-photocurrent device [19].

Zhu et al. built PV cells with the following architecture: (ITO)/poly (3,4-ethylenedioxythiophene):poly (styrenesulfonate) (PEDOT:PSS)/PM6: Y6/PNDIT-F3N-Br/Ag (conventional OPV cell) and achieved a peak efficiency of 16.88 %. Thermal annealing and the solvents C_6H_5Cl (CB) and $CHCl_3$ (CF) were utilized to modify the shape of the thin film. A PCE of 16.06 %, Jsc of 25.33 $mAcm^{-2}$, FF of 74.39%, and Voc of 0.852 V were obtained using CF with 0.5 % $C_{10}H_7Cl$ as a supplement. The attained values were Voc of 0.835 V, PCE of 16.88 %, Jsc of 26.52 $mAcm^{-2}$, and FF of 76.21% for the thermally annealed OPV cell at 80 °C. The CB's device, in contrast, had a lower PCE of 12.15 %, Jsc of 21.16 $mAcm^{-2}$, FF of 72.15 %, and Voc of 0.796 V [20].

Lin et al. studied the utilization of Benzyl Viologen (BV) for the development of further conceivable bulk hetero junction (BHJ) systems. This study experimented with five different blends which are PM6:Y6:PC71BM, (PTB7-Th):PC71BM, (PTB7-Th):EH-IDTBR, PM6:IT-2Cl, and PM6:Y6. These mixtures were also treated with BV (0.4 and 0.04 %) and without BV. The OPV cells based on PM6:Y6 (16.0 %) and PM6:Y6:PC71BM (17.1 %) deliver the best results. Finally, these investigations indicated that directly injecting minor amounts of BV (n-type) into the BHJ layer of OPV cells regularly enhances performance [21].

Moreover, Lin et al. also emphasise the need for research on Diquant (DQ) as a viable dopant for the usage in cutting-edge organic solar cells. In the analysis, DQ was introduced to PM6:Y6: PC71BM (ternary BHJ cells) and observed the PCEs were enhanced from 16.7 % to 17.4 %. Finally, in this research, DQ was applied to PM6:BTP-eC9:PC71BM, which was utilized as the dynamic layer in OPV cells, bringing about a most extreme uncertified PCE of 18.3% [22].

Likewise, Zhang et al. adjusted the electronic and morphological structure of the PM6:Y6 (active layer) to reach a PCE of 18.07 %. An ITO/PEDOT:PSS/Dynamic layer/ poly-fluorene-alt-naphthalene diimide-Br/Silver was used to make PV cells. At Voc = 0.842 V and Jsc = 25.98 $mAcm^{-2}$, the highest PCE of PM6:Y6 binary OPV devices was found to be 16.52 % with an FF of 75.52 %. Ternary devices with active layer blends PM6:PM7:Y6 had the highest PCE of17.02 %, FF of 76.70 %, Jsc of 26.17 $mAcm^{-2}$, and Voc of 0.848 V. Quaternary device with active layer blends PM6:PM7:Y6:PC71BM achieved a maximum PCE of 18.07 % with a Jsc of 26.55 $mAcm^{-2}$, and a Voc of 0.859 V along with FF of 79.23 %. Quaternary devices had a certified PCE = 17.35 % [23].

Furthermore, Guo et al. summarizes the current improvement in OPV cells using PM6:Y6. The modification of active layer is thoroughly discussed, including the incorporation of a triennial monomer into PM6 to produce a terpolymer. This research also looks at the evolution of ternary and quaternary devices, as well as different processing methods. The later section in this review summarizes and discusses the creation of electrode material and interfacial layers in PM6:Y6 (OPV cells). In conclusion, higher performing and commercially feasible OPV cells are likely to be available shortly as a result of combining these optimization methodologies, which were also mentioned [5].

Table 1 below provides the overall summary of the above particularized research works pertaining to different photovoltaic characteristics of the PM6:Y6 driven OPV cells used and the results attained thereof:-

Table 1. PV cell aspects of PM6:Y6

Active layer	Processing conditions	V_{OC} [V]	J_{SC} [mAcm^{-2}]	Fill Factor [FF %]	PCE [%]	Ref.
PM6:Y6 (N)	without	0.86	24.3	73.2	15.3	[14]
PM6:Y6 (N)	0.5% CN annealed at 110^{o}C	0.83	25.3	74.8	15.7	[14]
PM6:Y6 (I)	without	0.82	25.2	76.1	15.7	[14]
PM6:Y6 (N)	without	0.825	25.2	74	>15	[15]
PM6:Y6 (N)	0.01 wt% BCF	0.84	25.96	73.47	16.0	[16]
PM6:Y6 (N)	0.2 $PC_{71}BM$	0.848	24.5	74.6	15.5	[17]
PM7:Y6 (N)	0.2 $PC_{71}BM$	0.875	24.2	72.8	15.4	[17]
PM6:Y6:$PC_{71}BM$ (N)	0.2 $PC_{71}BM$	0.861	25.1	77.2	16.7	[17]
PM7:Y6:$PC_{71}BM$ (N)	0.2 $PC_{71}BM$	0.884	24.6	74.6	16.2	[17]
PM6:Y6 (N)	2 wt% PIDTC-T	0.847	25.50	77.6	16.8	[18]
PM6:Y6 (N)	CB 80^{o}C	0.796	21.16	72.15	12.2	[20]
	CF 80^{o}C	0.835	26.52	76.21	16.9	[20]
PM6:Y6:$PC_{71}BM$ (N)	0 wt% BV	0.84	25.7	75	16.3	[21]
	0.004 wt% BV	0.84	26.3	77	17.1	[21]
	0.4 wt% BV	0.83	25.3	67	14.2	[21]
PM6:Y6 (N)	0 wt% BV	0.83	25.1	73	15.3	[21]
	0.004 wt% BV	0.83	26.0	74	16.0	[21]
	0.4 wt% BV	0.82	24.3	66	13.1	[21]
PM6:IT-2Cl (N)	0 wt% BV	0.89	20.8	72	13.3	[21]
	0.004 wt% BV	0.89	22.0	73	14.3	[21]
	0.4 wt% BV	0.86	19.1	64	10.4	[21]
PTB7-Th:EH-IDTBR (N)	0 wt% BV	1.02	15.9	57	9.1	[21]
	0.004 wt% BV	1.02	16.4	60	9.9	[21]
	0.4 wt% BV	1.01	15.6	52	8.1	[21]
PTB7-Th:$PC_{71}BM$ (N)	0 wt% BV	0.80	17.5	65	9.0	[21]

	0.004 wt% BV	0.80	18.2	66	9.6	[21]
	0.4 wt% BV	0.78	16.9	61	8.0	[21]
PM6:Y6:PC71BM (N)	without	0.860	25.64	75.7	16.7	[22]
	0.01 wt% DQ	0.862	26.48	76.1	17.4	[22]
PM6:IT-4F (N)	without	0.856	20.34	74.9	13.0	[22]
	0.02 wt% DQ	0.862	21.98	75.7	14.3	[22]
PM6:BTP-eC9:$PC_{71}BM$ (N)	without	0.855	26.21	77.7	17.4	[22]
	0.01 wt% DQ	0.856	26.98	79.4	18.3	[22]
PM6:Y6 (N)	without	0.842	26.21	75.52	16.52	[23]
PM6:PM7:Y6 (N)	without	0.848	26.93	76.70	17.02	[23]
PM6:PM7:Y6:$PC_{71}BM$ (N)	without	0.859	26.55	79.23	18.07	[23]
PM7:Y6 (N)	without	0.879	24.89	69.10	15.12	[23]

Note: (N) – Normal topology, (I) – Inverted topology

3. PIF8BT-PDI BASED OPV CELLS

Perylene diimide (PDI) ought to be a promising candidate to replace fullerene in OPVs since PDI (n-type) organic semiconductor has excellent warm (thermic), light, and synthetic (chemical) stabilities. Furthermore, because of their remarkable electron mobility and very much positioned LUMO (ca.-4.0 eV) energy, these types of materials often exhibit considerable absorption in the visible or even NIR range, as well as high electron-tolerating ability. By altering their self-assembly, optoelectronic, and solvency characteristics, they could be analysed thoroughly. The PDI has been shown to be a conceivable acceptor of OPV cells. The proficiency of mono-PDI frameworks can accomplish up to 3 %. Because of the total brought about by the π–π (intermolecular) interaction, Mono-PDI derivatives perform poorly in general. To the anchorage of the PDI, different alkyl chains were added to overcome this problem [25].

Keivanidis et al. studied on PIF8BT:PDI and F8BT:PDI based OPVs. Figure 3 shows subatomic structure of donor PIF8BT and acceptor PDI. The study investigated how the efficiency photocurrent generation and kinetics of nonpaired charge recombination was related. The electrical and photophysical qualities of the aforementioned mixtures were accounted for. These findings suggest that the delayed luminescence that is induced by the kinetics of free carrier recombination can be used to indirectly monitor charge transport in a blend of FMs. For the preceding mixing functions, these dynamics are temperature sensitive and have a power-law decay function [24]. From 2012 to 2019, no work was found done in PIF8BT:PDI.

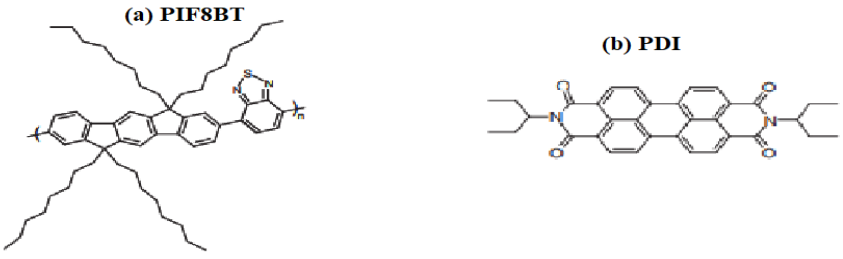

Figure 3. (a) Donor PIF8BT subatomic structure [24]. (b) Acceptor PDI subatomic structure [24].

Keivanidis et al. introduced a new delayed luminescence spectroscopy approach. Traps aid in the segregation of spatially isolated charge transporters and charge recombination in the proposed technique. It screens the postponed glow phosphorescence of mass heterojunctions with PDI cognate (acceptor) and PIF8BT (donor) using a quasi-time-integrated detection method. Thermal annealing produced an amalgam (PIF8BT:PDI) with four distinct microstructures. When PIF8BT:PDI is thermally annealed, the PDI domains shrink in tandem with the PIF8BT spaces in the mix. In this examination, for fast screening of a wide extension OPV amalgam with less exploratory intricacy at sensible expense, the delayed luminescence approach could turn into a significant symptomatic device. The suggested approach requires a moderate amount of equipment, is scalable to most device manufacturing facilities, and, most significantly, may be extended to other time-gated electroluminescence investigations [26].

Farooq et al. studied a new structure in which the photoactive absorber layer is PIF8BT (poly (9, 9dioctylindenofluorenecobenzothiadiazole)):PDI (N′bis (1ethylpropyl) 3, 4, 9, 10perylene tetracarboxy diimide). To improve cell assimilation and PCE, research has been conducted on various electrode materials such as fluorine tin oxide (FTO), Au, indium tin oxide, Ag and aluminium (Al) in various combinations with window layer materials such as titanium dioxide (TiO2) and ZnO. In this study the best presentation boundaries including FF of68.86 %, Voc of 0.59 V, PCE of 3.86 % and Jsc of 9.26 mA/m^2 were attained by utilizing ITO (top anode) and Al (bottom cathode) in the OPV structure with a similar dynamic material (PIF8BT:PDI) and different window and terminal materials [27].

Usman et al. used the following components: ITO/Spiro-MeOTAD/Active layer/Al to make OPV cells. The effect of photoactive layer thickness, different electrode pairs, different active layers, varied density of states (DOS) of the active layer, different hole conductive materials, and ultimately optimal performance of OPV with multiple active layers were explored in this study. The OPV cell with active layer PIF8BT:PDI obtained a Jsc of 125.51 Am^{-2}), Voc of 0.63V, an FF of 79.86 %, and a PCE of 6.35 % in this study [3].

4. PBDB-T_ITIC BASED OPV CELLS

In the recent age of OPV cells, the ITIC, an NFA, has garnered substantial interest[30][31][32][33]. Having a large number of backbones that are consistently coupled and electrons pulling out end groups, ITIC's with sub-atomic engineering (A-D-A) facilitate intramolecular transport and delocalization of charge carriers [34]. Figure 4 shows subatomic structure of donor PBDB-T and acceptor ITIC. Hou et al. found that the crystallinity of halogenated ITIC can be adjusted by the area of halogen atoms. During the research, it was discovered that chlorination outperforms fluorination in terms of broadening the absorption range and settling sub-atomic energy levels [33] [29] [34]. According to Lu et al., the PBDB-T (donor) and ITICs bis-subbed halogenation (F, Cl, and Br) as acceptors, the fluorinated framework created the most elevated Jsc, while the brominated framework delivered the most noteworthy FF (≈ 0.71%) with a limited quantity of corral region in the mixed film, bringing about a decrease in EQE and Jsc [34][28].

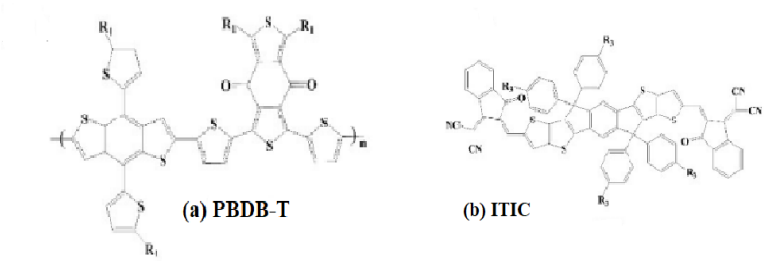

Figure 4. (a) Donor PBDB-T subatomic structure [28] (b) Acceptor ITIC sub atomic structure [29]

Zhao et al. did an experiment using PBDB-T:PC71BM and a polymer (PBDB-T:poly [(2,6-bis(4,8-bis(5-(2-ethylhexyl) thiophen-2-yl)-benzo[1,2-b: 4,5-b'] dithiophene]) 5,5-(1',3'-di-2-thienyl-5',7'-bis(2-ethylhexyl)benzo [1',2'-c:4',5'-c'] dithiophene-4,8-dione]) and small molecular compound (ITIC:3,9-bis(2-methylene-(1,1-dicyanomethylene)-indanone) -dithieno [2,3-d:2', 3'-d'] -s-indaceno [1,2-b:5,6-b'] dithiophene)". According to the findings, the optical absorption of the hybrid pellicle (PBDB-T/PC71BM) is not significantly superior to that of the hybrid pellicle (PBDB-T/ITIC). The study also investigated the absorption spectra's temperature-reliance of PBDB-T in the CB (chlorobenzene) arrangement. Here, a device structure (ITO/ZnO/BHJ-layer/MoO3/Al) was fabricated and found to yield a PCE of 7.45 %, Voc of 0.853 V, Jsc of 12.80 mAcm2, and an FF of 0.682 % utilizing PBDB-T:PC 71 BM (active layer). The FF of 0.742 %, Jsc of 16.80 $mAcm^{-2}$, Voc of 0.899 V, and PCE of 11.21 % were accomplished using PBDB-T:ITIC (active layer) [35].

Zhang et al. created a gadget using an inverted framework (ITO/ZnO/active layer/MoOx/Ag). The materials used in this review were N2200, PBDB-T and ITIC with bandgaps of 0.4 eV, 1.81 eV and 0.3 eV, respectively. On the OPV cell, the dynamic layer materials PBDB-T:N2200 and PBDB-T/ITIC were used. For the devices with PBDB-T/N2200, PCE was 6.33 %, with an FF of 64 %, a Jsc of 11.63 $mAcm^{-2}$ and a Voc of 0.85V [36].

Nian et al. made two profoundly productive ternate NFA PV cells with (more than 78 %) FFs and PCEs of up to 13.52 % and 12.70 %, respectively, by utilizing a firmly conglomerating polymer P1 in regular PBDB-T/IT-M and PBDBT/ITIC non-fullerene mixes. In compared to the binary mixture, the ternary devices demonstrate much enhanced withdrawal and reduced recombination of charges. The efficiency and fill factors of PBDB-T/ITIC (non-fullerene OPV) were 10.82 % and 70.85 % prior to adding P1. Subsequent to adding P1, the efficiency and fill factor ascend to 12.70 % and 78.07 %, respectively. In PBDB-T/IT-M (non-fullerene OPV), PCE ascends from 11.71 % to 13.52 %, and FF ascends from 72.07 % to 77.83 % [37].

Wang et al. synthesized a dual amalgam of PBDB-T:ITIC system. The study used an OPV with an upturned arrangement [glass/Indium Tin Oxide (180 nm)/Zinc oxide (ETL) (10 nm)/binary blend [PBDB-T: ITIC BHJ (90 nm)]/MoO3 (Molybdnum trioxide) (2 nm)/Ag (100 nm)], and a classic arrangement [glass/Indium Tin Oxide (180 nm)/PEDOT: PSS (HTL) (30 nm)/PBDBT: ITIC BHJ (110 nm)/ZnO (ETL) (20 nm)/Ag (100 nm)]. The results indicated that the PCE of the inverted structure is somewhat higher than that of the conventional configuration. PCE of 9.83 %, FF of 68.20 %, Jsc of 16.10 $mAcm^{-2}$, and Voc of 0.90V of inverted structure as well as PCE of 9.68 %, Jsc of 15.55 $mAcm^{-2}$, FF of 67.23 %, and Voc of 0.90 V of conventional structure were noted [38].

Zhang et al. studied three BHJ OPV cells: PBDB-T (donor) mixed with ITIC, N2200 and PCBM to evaluate photovoltaic performance and charge transfer. An up down arrangement ITO (Indium tin oxide)/ZnO(Zinc oxide)/PBDB-T/Acceptor/MoO3 (Molybdenum trioxide)/Ag was built and evaluated. The PBDB-T employed has -5.26 eV (HOMO) and -3.46 eV (LUMO). The HOMO levels

of N2200, PCBM, and ITIC were -5.77 eV, -5.92 eV, and -5.71 eV, respectively. In the interim, the LUMO levels were -4.32 eV, -4.10 eV, and -4.13 eV. The standard PCBM-fabricated devices had a PCE of 5.88%, Voc of 0.875V, FF of 65.1%, and Jsc of 10.34 $mAcm^{-2}$. PBDB-T: ITIC (OPV cell) has a marginally better Voc of 0.910 V, a considerably enhanced Jsc of 16.10 $mAcm^{-2}$, a marginally higher FF of 68.7 %, and the best PCE of 10.06 %. In conclusion, PBDB-T:N2200 has a comparable Voc of 0.865 V, a slightly enhanced Jsc of 11.67 $mAcm^{-2}$, and a similar FF of 66.1% [39].

Zhang et al. used blade-covering to create binary and ternary (PBDB-T:ITIC:FOIC) OPV cells. The study showed an enhancement of current density from 15.6 to 17.2 $mAcm^{-2}$ when FOIC introduced. The standard OPV cell arrangement [ITO (indium tin oxide) /PEDOT:PSS/Ternary blend (PBDB-T/ITIC/FOIC)/ZrAcac/ (Aluminium) Al] was utilized. The HOMO and LUMO values of ITIC, FOIC along with PBDB-T used in the review are -5.51/-3.78 eV, -5.36/-3.92 eV and -5.33/-2.92 eV. A PCE of 9.32 % was attained, as well as an FF of 66.6 %, Voc of 0.90 V and Jsc of 15.6 $mAcm^{-2}$. The device with active layer (PBDB-T: FOIC) on the other hand, has a substantially higher Jsc of 22.5 $mAcm^{-2}$ due to its wide absorption spectrum. However, the Voc of 0.72 V and FF of 61.8 % were relatively small, which led to a PCE of 9.91 %. The OPV cell with an active layer PBDB-T: ITIC, has more Voc than the optimized PBDB-T: ITIC: FOIC cell with a Voc of 0.89 V. However, because of the improved light-harvesting, the Jsc rose dramatically to 17.2 $mAcm^{-2}$. Furthermore, a significant FF of 69.8 % was reached at the maximum PCE of 10.68%. Additionally, the adjustable large area PBDB-T: ITIC: FOIC cell of 105 mm^2 arrangement produced a Voc of 0.88 V, an FF of 66.8 %, a huge PCE of 9.81 %, and a Jsc of 16.7 $mAcm^{-2}$ [40].

Arredondo et al. examined the performance by utilizing topology, PET (polyethylene terephthalate)/Ag/ZnO/ Binary blend (PBDB-T: ITIC)/FHCPEDOT: PSS. In the study, fabrication of OPV cells was made using air-refined slot-die coating on an ITO free substrate by incorporating and not incorporating 1,8-diiooctane (DIO) additive. OPV cell with DIO got a PCE of 4.97 %, an FF of 52.7 %, a Voc of 0.811 V and a Jsc of 11.56 $mAcm^{-2}$, whereas OPV cell without DIO got a Jsc of 11.02 $mAcm^{-2}$, a PCE of 4.03 %, an FF of 46.6 % and a Voc of 0.783 V [41]. Table 2 below provides the overall summary of the above particularized research works pertaining to different photovoltaic peculiarities of PBDB-T/ ITIC driven Polymer PV Cells used and the results attained thereof:-

Table 2. PV cell aspects of PBDB-T/ITIC

Active layer	Processing conditions	V_{OC} [V]	J_{SC} [$mAcm^{-2}$]	Fill Factor [FF %]	PCE [%]	Ref.
PBDB-T/ ITIC (I)	without	0.88	14.68	70	9.1	[35]
PBDB-T/ ITIC (N)	0% P1	0.90	16.64	71.27	10.66	[37]
PBDB-T/ ITIC (N)	5% P1	0.90	17.98	77.33	12.51	[37]
PBDB-T/ ITIC (N)	10% P1	0.90	17.48	75.78	11.92	[37]
PBDB-T/ ITIC (N)	100% P1	0.93	8.15	54.44	3.85	[37]
PBDB-T/ ITIC (I)	without	0.90	16.10	68.20	9.83	[38]
PBDB-T/ ITIC (N)	without	0.90	15.55	67.23	9.68	[38]
PBDB-T/ ITIC (I)	without	0.910	16.10	68.7	10.06	[39]
PBDB-T/ ITIC (N)	without	0.90	15.6	66.6	9.32	[40]
PBDB-T/ITIC/FOIC (N)	without	0.89	17.2	69.8	10.68	[40]
PBDB-T/ FOIC (N)	without	0.72	22.5	61.8	9.91	[40]
PBDB-T/ ITIC (N)	DIO	0.811	11.56	52.7	4.97	[41]
PBDB-T/ ITIC (N)	Without DIO	0.783	11.02	46.6	4.03	[41]

Note: (N) – Normal topology, (I) – Inverted topology

5. PM6:Y6, PIF8BT:PDI and PBDBT:ITIC comparisons

An analogy between PM6:Y6, PIF8BT:PDI and PBDBT:ITIC (OPV cells) has additionally been done and has been kept in the Table 3 , which drives us to PM6:Y6 (quaternary) topology that showed the best PCE to date.

Table 3. An analogy of photovoltaic aspects between PM6:Y6, PIF8BT:PDI, and PBDB-T:ITIC-driven OPV cells

ASPECTS	PM6:Y6	PIF8BT:PDI	PBDB-T:ITIC
Reference	[23]	[3]	[38]
Power conversion efficiency (η)	18.07%	6.35%	12.51%
***Open-Circuit Voltage* [V_{OC} (V)]**	0.859	0.63	0.90
***Short-Circuit Current* [J_{SC} ($mAcm^{-2}$)]**	26.55	12.551	17.98
Fill Factor [FF (%)]	79.23	79.86	77.33
Topology used	Normal	Normal	Normal
Single, Binary, Ternary, Quaternary devices	Quaternary (PM6:PM7:Y6:$PC_{71}BM$)	Binary (PIF8BT:PDI)	Binary (PBDB-T: ITIC)
ETL material used	PFNDI-Br	Not used	MoO3
HTL material used	PEDOT:PSS	Spiro-MeOTAD	Zno
Processing conditions	Not used	Not used	5% P1 used
Bandgaps	PM6=1.85eV, PM7= 1.86, Y6=1.37	1.10eV	Not mentioned

6. CONCLUSIONS AND OUTLOOKS

The improvement of OPV cells as of late has brought a forward leap in the realm of PV cells. Scientists and researchers are developing new polymer compounds that improve power conversion efficiency. We focused on three novel active layer materials in this study of review paper: PM6Y6, PIF8BT:PDI, and PBDB-T:ITIC. According to this analysis, quaternary devices with active layer blends PM6:PM7:Y6:PC71BM achieved the highest PCE (18.07 %), the OPV cell with PIF8BT:PDI (active layer) achieved the highest PCE (6.35 %), and finally, PBDB-T/ ITIC-based OPV cell achieved maximal PCE (12.51 %) under certain processing conditions.

In ternary or quaternary device architectures, OPV cells with active layers PBDB-T:ITIC and PM6:Y6 exhibited substantial efficiency. With the inclusion of additional additive materials, the single junction PM6:Y6 based OPV cells demonstrated remarkable efficiency. There hasn't been much progress with PIF8BT:PDI-based OPV cells. Several factors must be examined in order to improve the performance of these OPV cells:

1) A fundamental OPV cell structure consists of a cathode, ETL, active layer, HTL, anode, and substrate. In this regard, appropriate cathode, anode, ETL, HTL, and substrate materials, as

well as correct thickness, can boost OPV cell efficiency. An active layer of the correct thickness also aids in performance enhancement.

2) To manage an active layer's morphology, there is an increased focus on creating the film by regulating the kinetics and thermodynamics during its evolution, along with the thermal transition of the molecules. For the augmentation of the active layer in solution-processed OPV cells, the methods of modifying the donor-acceptor ratio, solvent/thermal annealing, solvent selection, and solid/solvent additive processing are most often utilized.
3) More work in PIF8BT:PDI-based OPV cells are required, taking the abovementioned factors into account.
4) An itemized study connected with bandgaps of the previously mentioned materials is required in order to get great efficiency.

The OPV cell is predicted to be upscaled from lab to practical level with excellent efficiency by merging these optimization methodologies.

REFERENCES

[1] K. W. Böer, "Solar Cells," in Survey of Semiconductor Physics.Vol. II., New York: John Wiley., 2002. [Online]. Available: http://www.chemistryexplained.com/Ru-Sp/Solar-Cells.html

[2] O. K. Simya, P. Radhakrishnan, A. Ashok, K. Kavitha, and R. Althaf, "Engineered nanomaterials for energy applications," in Handbook of Nanomaterials for Industrial Applications, 2018, pp. 751–767. doi: 10.1016/B978-0-12-813351-4.00043-2.

[3] Yasir Usman et al., "Comparative Simulation-Based Study on Different Active Layers of," Sch J Eng Tech, vol. 9523, no. 8, pp. 113–119, 2021, doi: 10.36347/sjet.2021.v09i08.002.

[4] Jacob Marsh, "organic solar cells:what you need to know," energysage.com. https://news.energysage.com/organic-solar-cells-what-you-need-to-know (accessed Apr. 14, 2022).

[5] Q. Guo et al., "Recent advances in PM6:Y6-based organic solar cells," Mater. Chem. Front., vol. 5, no. 8, pp. 3257–3280, 2021, doi: 10.1039/d1qm00060h.

[6] E. Becquerel, "Comptes rendus hebdomadaires des séances de l'Académie des sciences / publiés... par MM. les secrétaires perpétuels.," A. A. des Sci. (France). A. du., 1839, [Online]. Available: https://gallica.bnf.fr/ark:/12148/bpt6k2968p/f562.item%0A

[7] Smith, "Effect of Light on Selenium During the Passage of An Electric Current*," Nature, vol. 7, no. 173, p. 303, 1873, doi: 10.1038/007303e0.

[8] A. Pochettino, A. and Sella, "Photoelectric behavior of anthracene.," Acad. Lincei Rend, 15, pp.355-363., 1906.

[9] D. Keaens and M. Calvin, "Photovoltaic effect and photoconductivity in laminated organic systems," J. Chem. Phys., vol. 29, no. 4, pp. 950–951, 1958, doi: 10.1063/1.1744619.

[10] A. K. Ghosh, D. L. Morel, T. Feng, R. F. Shaw, and C. A. Rowe, "Photovoltaic and rectification properties of Al/Mg phthalocyanine/Ag schottky-barrier cells," J. Appl. Phys., vol. 45, no. 1, pp. 230–236, 1974, doi: 10.1063/1.1662965.

[11] S. Glenis, G. Tourillon, and F. Garnier, "Influence of the doping on the photovoltaic properties of thin films of poly-3-methylthiophene," Thin Solid Films, vol. 139, no. 3, pp. 221–231, 1986, doi: 10.1016/0040-6090(86)90053-2.

[12] R. H. Halls, J. J. M., & Friend, "The photovoltaic effect in a poly (p-phenylenevinylene)/peryleneheterojunction.," Synth. Met. 85(1-3), 1307-1308, 1997.

[13] E. (n. d.). Spooner, "Organic Photovoltaics: An Introduction.," Ossilla.com. https://www.ossila.com/en-in/pages/organic-photovoltaics-introduction#:~:text=References-,What is an OPV%3F,and double bonds) is required. (accessed Apr. 14, 2022).

[14] J. Yuan et al., "Single-Junction Organic Solar Cell with over 15% Efficiency Using Fused-

Ring Acceptor with Electron-Deficient Core," Joule, vol. 3, no. 4, pp. 1140–1151, 2019, doi: 10.1016/j.joule.2019.01.004.
[15] A. Karki et al., "Understanding the High Performance of over 15% Efficiency in Single-Junction Bulk Heterojunction Organic Solar Cells," Adv. Mater., vol. 31, no. 48, 2019, doi: 10.1002/adma.201903868.
[16] D. Zhang et al., "Control of Nanomorphology in Fullerene-Free Organic Solar Cells by Lewis Acid Doping with Enhanced Photovoltaic Efficiency," ACS Appl. Mater. Interfaces, vol. 12, no. 1, pp. 667–677, 2020, doi: 10.1021/acsami.9b17238.
[17] M. A. Pan et al., "16.7%-efficiency ternary blended organic photovoltaic cells with PCBM as the acceptor additive to increase the open-circuit voltage and phase purity," J. Mater. Chem. A, vol. 7, no. 36, pp. 20713–20722, 2019, doi: 10.1039/c9ta06929a.
[18] T. Yang et al., "A compatible polymer acceptor enables efficient and stable organic solar cells as a solid additive," J. Mater. Chem. A, vol. 8, no. 34, pp. 17706–17712, 2020, doi: 10.1039/d0ta06146h.
[19] N. Tokmoldin et al., "Extraordinarily long diffusion length in PM6:Y6 organic solar cells," J. Mater. Chem. A, vol. 8, no. 16, pp. 7854–7860, 2020, doi: 10.1039/d0ta03016c.
[20] L. Zhu et al., "Efficient Organic Solar Cell with 16.88% Efficiency Enabled by Refined Acceptor Crystallization and Morphology with Improved Charge Transfer and Transport Properties," Adv. Energy Mater., vol. 10, no. 18, 2020, doi: 10.1002/aenm.201904234.
[21] Y. Lin et al., "17.1% Efficient Single-Junction Organic Solar Cells Enabled by n-Type Doping of the Bulk-Heterojunction," Adv. Sci., vol. 7, no. 7, pp. 1–9, 2020, doi: 10.1002/advs.201903419.
[22] Y. Lin et al., "A Simple n-Dopant Derived from Diquat Boosts the Efficiency of Organic Solar Cells to 18.3%," ACS Energy Lett., vol. 5, no. 12, pp. 3663–3671, 2020, doi: 10.1021/acsenergylett.0c01949.
[23] M. Zhang et al., "Single-layered organic photovoltaics with double cascading charge transport pathways: 18% efficiencies," Nat. Commun., vol. 12, no. 1, pp. 1–10, 2021, doi: 10.1038/s41467-020-20580-8.
[24] P. E. Keivanidis et al., "Correlating emissive non-geminate charge recombination with photocurrent generation efficiency in polymer/perylene diimide organic photovoltaic blend films," Adv. Funct. Mater., vol. 22, no. 11, pp. 2318–2326, 2012, doi: 10.1002/adfm.201102871.
[25] W. Chen, X. Yang, G. Long, X. Wan, Y. Chen, and Q. Zhang, "A perylene diimide (PDI)-based small molecule with tetrahedral configuration as a non-fullerene acceptor for organic solar cells," J. Mater. Chem. C, vol. 3, no. 18, pp. 4698–4705, 2015, doi: 10.1039/c5tc00865d.
[26] P. E. Keivanidis et al., "Afterglow Effects as a Tool to Screen Emissive Nongeminate Charge Recombination Processes in Organic Photovoltaic Composites," ACS Appl. Mater. Interfaces, vol. 12, no. 2, pp. 2695–2707, 2020, doi: 10.1021/acsami.9b16036.
[27] W. Farooq, A. D. Khan, A. D. Khan, and M. Noman, "Enhancing the power conversion efficiency of organic solar cells," Optik (Stuttg)., vol. 208, no. 03, pp. 94–97, 2020, doi: 10.1016/j.ijleo.2019.164093.
[28] S. Lu et al., "Halogenation on terminal groups of ITIC based electron acceptors as an effective strategy for efficient polymer solar cells," Sol. Energy, vol. 195, no. November 2019, pp. 429–435, 2020, doi: 10.1016/j.solener.2019.11.074.
[29] H. Zhang et al., "Over 14% Efficiency in Organic Solar Cells Enabled by Chlorinated Nonfullerene Small-Molecule Acceptors," Adv. Mater., vol. 30, no. 28, pp. 1–7, 2018, doi: 10.1002/adma.201800613.
[30] L. Benatto and M. Koehler, "Effects of Fluorination on Exciton Binding Energy and Charge Transport of -Conjugated Donor Polymers and the ITIC Molecular Acceptor: A Theoretical Study," J. Phys. Chem. C, vol. 123, no. 11, pp. 6395–6406, 2019, doi: 10.1021/acs.jpcc.8b12261.
[31] N. Y. Doumon et al., "Photostability of Fullerene and Non-Fullerene Polymer Solar Cells: The Role of the Acceptor," ACS Appl. Mater. Interfaces, vol. 11, no. 8, pp. 8310–8318,

2019, doi: 10.1021/acsami.8b20493.
[32] Y. Yang, "The Original Design Principles of the Y-Series Nonfullerene Acceptors, from Y1 to Y6," ACS Nano, vol. 15, no. 12, pp. 18679–18682, 2021, doi: 10.1021/acsnano.1c10365.
[33] Y. Zhang et al., "Fluorination vs. chlorination: a case study on high performance organic photovoltaic materials," Sci. China Chem., vol. 61, no. 10, pp. 1328–1337, 2018, doi: 10.1007/s11426-018-9260-2.
[34] Y. Wang et al., "The halogenation effects of electron acceptor itic for organic photovoltaic nano-heterojunctions," Nanomaterials, vol. 11, no. 12, pp. 1–19, 2021, doi: 10.3390/nano11123417.
[35] W. Zhao et al., "Fullerene-Free Polymer Solar Cells with over 11% Efficiency and Excellent Thermal Stability," Adv. Mater., vol. 28, no. 23, pp. 4734–4739, 2016, doi: 10.1002/adma.201600281.
[36] Y. Zhang et al., "Thermally Stable All-Polymer Solar Cells with High Tolerance on Blend Ratios," Adv. Energy Mater., vol. 8, no. 18, pp. 1–10, 2018, doi: 10.1002/aenm.201800029.
[37] L. Nian et al., "Ternary non-fullerene polymer solar cells with 13.51% efficiency and a record-high fill factor of 78.13%," Energy Environ. Sci., vol. 11, no. 12, pp. 3392–3399, 2018, doi: 10.1039/c8ee01564c.
[38] Y. Wang et al., "Stability of Nonfullerene Organic Solar Cells: from Built-in Potential and Interfacial Passivation Perspectives," Adv. Energy Mater., vol. 9, no. 19, pp. 1–9, 2019, doi: 10.1002/aenm.201900157.
[39] Q. Zhang et al., "Understanding the Interplay of Transport-Morphology-Performance in PBDB-T-Based Polymer Solar Cells," Sol. RRL, vol. 4, no. 4, 2020, doi: 10.1002/solr.201900524.
[40] L. Zhang et al., "Regulating crystallization to maintain balanced carrier mobility via ternary strategy in blade-coated flexible organic solar cells," Org. Electron., vol. 89, p. 106027, 2021, doi: 10.1016/j.orgel.2020.106027.
[41] B. Arredondo et al., "Influence of solvent additive on the performance and aging behavior of non-fullerene organic solar cells," Sol. Energy, vol. 232, no. January, pp. 120–127, 2022, doi: 10.1016/j.solener.2021.12.052.